ADAPTIVE SELF-INTERFERENCE SUPPRESSION FOR FULL-DUPLEX RELAYS WITH MULTIPLE RECEIVE ANTENNAS

*Emilio Antonio-Rodríguez**

Galician R&D Center in
Advanced Telecommunications (GRADIANT)
Vigo, Spain

*Roberto López-Valcarce**

Dept. Signal Theory & Communications
University of Vigo
Vigo, Spain

ABSTRACT

In full-duplex relays, simultaneous reception and transmission in the same frequency results in self-interference which distorts the retransmitted signal and makes the relay prone to oscillation. We present an adaptive feedback canceller for multiple-input single-output (MISO) relays, efficiently combining spatial and temporal processing. The receive array is adaptively steered towards the minimum variance distortionless response (MVDR), whereas the temporal filter update is based on a novel low-complexity spectrum shaping scheme which avoids introducing additional delay in the relay station.

***Index Terms*—** Full-duplex, relays, adaptive algorithm, feedback cancellation, MISO, MVDR, spectrum shaping.

1. INTRODUCTION

Relays constitute a promising, cost-effective approach to extending wireless network coverage [1, 2] and to increasing network throughput by providing cooperative diversity [3, 4]. Relays may work in two different modes. In *half-duplex mode,* the relay transmits and receives by using two separate time slots and/or two different carrier frequencies. In spite of a reduction in spectral efficiency, this mode simplifies the design, since no coupling between transmission and reception is present. This spectral efficiency penalty vanishes in *full-duplex mode*, in which the relay receives at the same time and in the same frequency it transmits. However, this mode leads to coupling between the transmit and receive frontends. This self-interference problem is of utmost importance, since the power of the coupled signal can be much higher (tens of dB) than that of the signal coming from the transmitter, even with careful antenna isolation. Consequently, relays must include self-interference mitigation techniques [5, 6, 7]. Recently, a novel adaptive self-interference canceller for relays equipped with a single receive and a single transmit antenna has been proposed in [8]. In contrast with other methods [9], this scheme does not require the introduction of additional processing delay in the relay station, which is detrimental in multicarrier cyclic prefix-based networks. In this paper we extend this method to relays equipped with multiple receive antennas, in order to effectively combine spatial and temporal adaptive cancellation of the coupling signal.

In [10] a related approach is considered for relays with a single receive antenna and multiple transmit antennas. The transmit signals are prefiltered in order to minimize antenna coupling. This single-input, multiple-output (SIMO) configuration, however, has several drawbacks with respect its multiple-input, single-output (MISO) counterpart. The first one is the proliferation of high power amplifiers (HPAs) with the corresponding increase in power consumption. In addition, the effect of this pre-nulling in the final destination when channels are frequency-selective is not clear. Pefilter design in [10] is done off-line based on channel knowledge, although no specific channel estimation methods were proposed. Finally, the temporal canceller in [10], although adaptive, will present a bias when processing signals with colored power spectrum [8]. In contrast, our MISO approach is fully adaptive and can deal with arbitrary power spectra. It operates directly on waveform samples, and thus it is well suited for Amplify-and-Forward (A&F) relays. Although A&F relaying is not necessarily optimal, it is a flexible and popular scheme which has the advantage of being transparent to the specific modulation type of the transmitted signal [11].

The paper is organized as follows. The system model is set forth in Sec. 2. The proposed adaptive algorithm is presented in Sec. 3 and stationary point properties are investigated in Sec. 4. Sec. 5 shows simulation results, and conclusions are drawn in Sec. 6.

2. PROBLEM SETTING

Fig. 1 schematically shows a MISO A&F full-duplex relay. Among all of its components, the most important are:

- The M receive analog front-ends, each comprising a receive antenna and a down-conversion stage to interme-

*Supported by the European Regional Development Fund (ERDF) and the Spanish Government under projects DYNACS (TEC2010-21245-C02-02/TCM) and COMONSENS (CONSOLIDER-INGENIO 2010 CSD2008-00010), and the Galician Regional Government under projects ESCOLMA (10TIC013CT) and "Consolidation of Research Units" 2009/62 and 2010/85.

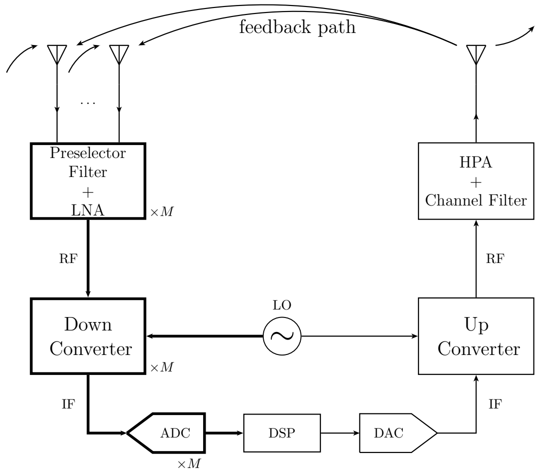

Fig. 1. MISO wireless relay. The relay has M reception antennas and one transmission antenna.

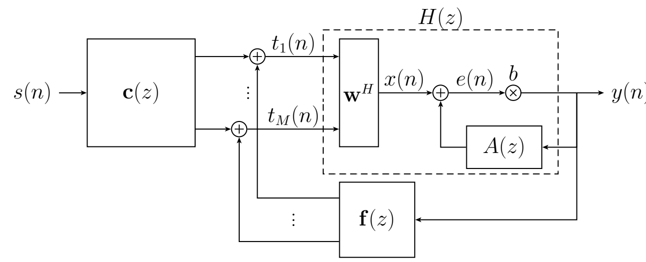

Fig. 2. Equivalent baseband system.

diate frequency (IF, which can be zero) . We consider a one-dimensional uniform linear array (ULA).

- The digital stage consisting of the M analog-to-digital converters (ADC), a digital signal processing (DSP) unit, and the corresponding digital-to-analog device (DAC). The underlying sampling rate is $f_s = 1/T_s$.
- The transmit analog front-end, comprising the up-conversion stage to RF, a high-power amplifier, a channel filter to reduce out-of-band emissions and the transmit antenna. The down- and up-conversion stages are controlled by a common local oscillator (LO).

We now describe the equivalent discrete-time system from the point of view of the DSP unit, which will include the space-time feedback supressor (STFS) whose design is our main goal. The incoming signal from the source, whose bandwidth is assumed much smaller than the carrier frequency, is denoted by $s(n)$. It is assumed that the transmitter has a single antenna and that channel time variations can be neglected in a first approximation[1], so that the transmitter-to-relay channel can be modeled as [12]:

$$\boldsymbol{d}(\omega) = \sum_{i=0}^{N_p-1} \beta_i \boldsymbol{v}(\theta_i^{(s)}) e^{-j\omega\Delta_i/T_s}, \tag{1}$$

where N_p is the number of propagation paths, and β_i and Δ_i are the gain and delay of each path, respectively. Each path has an associated phase $\theta_i^{(s)}$ (the transmitter-to-relay direct path corresponds to the term $\beta_0 \mathbf{v}(\theta_0^{(s)}) e^{j\omega\Delta_0}$), and the (normalized) ULA response is [13]

$$\boldsymbol{v}(\theta) = \frac{1}{\sqrt{M}} \left[\begin{array}{cccc} 1 & e^{j\theta} & \cdots & e^{j(M-1)\theta} \end{array} \right]^H, \tag{2}$$

where $\theta = \frac{2\pi d}{\lambda} \sin\phi$, with λ, d and ϕ respectively the carrier wavelength, element separation and broadside arrival angle.

Similarly to (1), the coupling channel between the transmit antenna and the receive array is modeled as:

$$\boldsymbol{p}(\omega) = \sum_{i=1}^{N_e} \rho_i \boldsymbol{v}(\theta_i^{(r)}) e^{-j\omega\Phi_i/T_s}, \tag{3}$$

where N_e is the number of feedback paths, and ρ_i and Φ_i are the gain and delay of each feedback path, respectively. We will denote by $\boldsymbol{d}(z) = \sum_{i=0}^{L_d} \boldsymbol{d}_i z^{-i}$ and $\boldsymbol{p}(z) = \sum_{i=1}^{L_p} \boldsymbol{p}_i z^{-i}$ the z-domain versions of (1) and (3) respectively.

The discrete-time representation of the j-th analog frontend at the receive side is denoted by the transfer functions $G_j(z)$, $j = 1,\ldots,M$; whereas that of the analog frontend at the transmit side is denoted by $V(z)$. We denote by $\boldsymbol{h}(z)$ the M-input, single-output STFS transfer funcion.

Fig. 2 represents the baseband equivalent system of the relay from the STFS perspective, where we have introduced the equivalent source-to-relay and coupling transfer functions $\boldsymbol{c}(z) = \boldsymbol{G}(z)\boldsymbol{d}(z)$ and $\boldsymbol{f}(z) = \boldsymbol{G}(z)\boldsymbol{p}(z)V(z)$ respectively, with

$$\boldsymbol{G}(z) = \mathrm{diag}\left\{ \begin{array}{ccc} G_1(z) & \cdots & G_M(z) \end{array} \right\}. \tag{4}$$

The STFS consists of a spatial processing block (linear combiner) $\boldsymbol{w} = \left[\begin{array}{ccc} w_1 & \cdots & w_M \end{array} \right]^T$ followed by the temporal processing block (an adaptive infinite impulse response (IIR) filter) with transfer function $\frac{b}{1-bA(z)}$ with $A(z) = \sum_{j=1}^{L_a} a_j z^{-j}$, and whose output is denoted $y(n)$. The transfer function of the overall system $K(z)$ from $s(n)$ to $y(n)$ is therefore

$$K(z) = \frac{b\boldsymbol{w}^H \boldsymbol{c}(z)}{1 - b[\boldsymbol{w}^H \boldsymbol{f}(z) + A(z)]}. \tag{5}$$

The feedback effect shows clearly in the denominator of (5). Intuitively, if the receive front-end transfer functions are reasonably close, i.e. $G_i(z) \approx G(z)$ for $i = 1,\ldots,M$, then

[1]The adaptive algorithms presented in the sequel should be able to track time variations in the operating environment, provided that these are sufficiently slow.

the self-interference could be supressed by spatial processing alone by choosing $\boldsymbol{w}^H \boldsymbol{v}(\theta_j^{(r)}) = 0$, $1 \leq j \leq N_e$. However, if the number of feedback paths is large, the degrees of freedom in $\boldsymbol{w}$ may not be sufficient. But note that by choosing $A(z) = -\boldsymbol{w}^H \boldsymbol{f}(z)$, the self-interference is completely canceled. Thus the combination of spatial and temporal processing offers additional flexibility in order to effectively suppress the coupling effect. Note that the order of $A(z)$ must be at least as large as that of $\boldsymbol{f}(z)$, i.e. the time span of the STFS should be comparable to the closed-loop delay of the feedback path.

3. ADAPTIVE ALGORITHM FOR SELF-INTERFERENCE SUPPRESSION

Spatial processing allows to discriminate signals based on the incoming direction, thus providing additional isolation between reception and transmission. We assume that the direction of arrival of the desired signal, and therefore $\theta_0^{(s)}$, is known[2]. Hence, a suitable criterion for the adaptation of $\boldsymbol{w}$ is the minimization of the power of the array output $x(n)$, subject to a unity gain constraint on the desired direction:

$$\min_{\boldsymbol{w}} \mathbb{E}\{|x(n)|^2\} \qquad \text{s. t.} \quad \boldsymbol{w}^H \boldsymbol{v}(\theta_0^{(s)}) = 1. \tag{6}$$

The solution of (6) is the Minimum Variance Distortionless Response (MVDR) beamformer, and accordingly $\boldsymbol{w}$ can be updated using (among other possibilities) Frost's rule [15]:

$$\boldsymbol{w}(n+1) = \boldsymbol{w}_s + \boldsymbol{P}\left[\boldsymbol{w}(n) - \mu_w \boldsymbol{t}(n) x^*(n)\right], \tag{7}$$

with $\boldsymbol{t}(n) = \begin{bmatrix} t_1(n) & \cdots & t_M(n) \end{bmatrix}^T$ the input vector (cf. Fig. 2), $\boldsymbol{w}_s = \boldsymbol{v}(\theta_0^{(s)})$ the initialization vector, $\boldsymbol{P} = \boldsymbol{I} - \boldsymbol{w}_s \boldsymbol{w}_s^H$ the projection matrix, and μ_w the learning rate.

As mentioned earlier, spatial processing alone may not be sufficient to deal with high-power coupling signals, because the attenuation caused by the beamformer $\boldsymbol{w}$ could be not enough to fully suppress these interferers. Additionally, with a small number of antennas, the angle resolution provided by the array may be too coarse. Thus we advocate the use of the temporal processing block, which can suppress the remaining self-interference in the system. In our case, as shown in the system layout of Fig. 2, this block cancels self-interference by identifying the feedback path $\boldsymbol{w}^H \boldsymbol{f}(z)$. The adaptive algorithm from [8] will be employed to this end:

$$\begin{aligned} b(n+1) &= b(n) + \mu_b (r_0 - |y(n)|^2), & (8)\\ a_k(n+1) &= a_k(n) + \mu_a [r_k - y(n) y^*(n-k)]. & (9) \end{aligned}$$

The constants r_k, $0 \leq k \leq L_a$ are set to match the autocorrelation of the desired signal $s(n)$ up to an irrelevant scaling, i.e. $r_k = c^2 \cdot \mathbb{E}\{s(n) s^*(n-k)\}$ for some $c^2 > 0$. Knowledge of $\{r_k\}$ can reasonably be assumed in practice, given the modulation format and parameters employed by the network. As discussed in [8], the introduction of these constants in the adaptive rule (8)-(9) has the effect of avoiding the bias that would otherwise take place when the desired signal is not temporally white. Moreover, this is done without introducing additional delay in the relay station as in other approaches [9]. Intuitively, (8)-(9) is effectively shaping the power spectrum of the output $y(n)$ in order to match that of $s(n)$; thus, in addition to eliminating self-interference, the STFS also has the capability of compensating in part for source-to-relay multipath effects (this capability is limited to minimum phase channels, since the adaptive algorithm is based on second-order statistics alone).

[2] The angle $\theta_0^{(s)}$ can be estimated beforehand using techniques from [14] in an initial training phase in which the relay remains quiet to avoid feedback.

4. STATIONARY POINTS

I order to investigate the stationary points $(\boldsymbol{w}_\star, b_\star, A_\star(z))$ of the update scheme described in Sec. 3, consider first the adaptation rule (7). It is readily seen that by taking $\boldsymbol{w}(0) = \boldsymbol{w}_s$ so that $\boldsymbol{w}^H(0)\boldsymbol{w}_s = 1$, this property remains invariant along the iterations, i.e. $\boldsymbol{w}^H(n)\boldsymbol{w}_s = 1$ for all n. Using this fact, it follows that at any stationary point $\boldsymbol{w}_\star$ must satisfy

$$\boldsymbol{w}_\star = (\boldsymbol{w}_s^H \boldsymbol{R}_{tt} \boldsymbol{w}_s)^{-1} \boldsymbol{R}_{tt}^{-1} \boldsymbol{w}_s, \tag{10}$$

where $\boldsymbol{R}_{tt} = \mathbb{E}\{\boldsymbol{t}_\star(n) \boldsymbol{t}_\star^H(n)\}$, and $t_\star(n)$ is the input vector attained at the stationary point. Eq. (10) is the expression of the MVDR beamformer for an input vector $\boldsymbol{t}_\star(n)$ [15].

On the other hand, by design the output autocorrelation at the stationary point must satisfy

$$\mathbb{E}\{y(n) y^*(n-k)\} = c^2 \cdot \mathbb{E}\{s(n) s^*(n-k)\} \quad 0 \leq k \leq L_a. \tag{11}$$

Let $\mathsf{S}_s(z)$ and $\mathsf{S}_y(z)$ denote the power spectral densities of $s(n)$ and $y(n)$ respectively, and note that these are related by $\mathsf{S}_y(z) = K_\star(z) K_\star^*(1/z^*) \mathsf{S}_s(z)$, where $K_\star(z)$ is the overall transfer function at the stationary point, see (5). If the adaptive filter order L_a is sufficiently large, we can translate the time-domain conditions (11) into the frequency domain as $\mathsf{S}_y(z) = c^2 \mathsf{S}_s(z)$. It follows that $K_\star(z)$ is an allpass function. If $\boldsymbol{w}_\star^H \boldsymbol{c}(z)$ is minimum phase, then we can conclude that $K_\star(z) K_\star^*(1/z^*) = c^2$ implies

$$K_\star(z) = \frac{b_\star \boldsymbol{w}_\star^H \boldsymbol{c}(z)}{1 - b_\star[\boldsymbol{w}_\star^H \boldsymbol{f}(z) + A_\star(z)]} = c \cdot z^{-\delta} \tag{12}$$

for some delay δ, i.e. the allpass function must reduce to a pure delay. This means that the STFS has achieved self-interference cancellation as well as multipath compensation.

5. SIMULATION RESULTS

We present an illustrative example of the behavior of the adaptive STFS proposed. In the simulation setting, the samples $s(n)$ correspond to those of a baseband single-carrier

16-QAM waveform with square-root raised cosine pulse shaping, roll-off factor $\alpha = 1$ and baud rate 5 Msymbols/s. The sampling frequency is $f_s = 10$ Msamples/s. Fig. 3 shows the power spectral density of $s(n)$ (normalized to unit power), together with the corresponding values of its autocorrelation sequence $|r_k|$. Regarding the channel $\boldsymbol{d}(\omega)$, we use 2 paths for the link between transmitter and the relay with the following parameters:

$$\beta_0 = 1, \quad \Delta_0 = 1\,\mu\text{s}, \quad \theta_0^{(s)} = 0, \tag{13}$$

$$\beta_1 = 0.75, \quad \Delta_1 = 1.2\,\mu\text{s}, \quad \theta_1^{(s)} = 0.0556\pi. \tag{14}$$

We consider an array with $M = 3$ antennas with separation $d = \lambda/2$ and set $G_i(z) = 1$ for $i = 1,2,3$. The resulting transfer functions from $s(n)$ to the STFS input are shown in Fig. 4. Significant frequency nulls can be observed as a result of multipath propagation.

The transmit analog frontend is modeled as a pure delay of 1.6 μs which summarizes the overall delay of the analog filters in the relay station: thus $V(z) = z^{-16}$. The number of feedback paths is 2. We neglect the effect of the propagation delay in the feedback path $\boldsymbol{p}(z)$ (i.e. $\Phi_1 = \Phi_2 \approx 0$), since in a typical set-up with transmit and receive antennas separated by less than 15 m, such delay accounts for less than half a sample period at $f_s = 10$ MHz. The remaining parameters of the feedback channel are:

$$\rho_0 = 1, \quad \theta_{r_0} = 0.1111\pi, \tag{15}$$

$$\rho_1 = 0.8, \quad \theta_{r_1} = -0.1833\pi. \tag{16}$$

Spatially and temporally white Gaussian noise is added at the STFS inputs in order to yield a Signal-to-Noise Ratio (SNR) of 25 dB. The adaptive filter has $L_a = 16$ taps, and the step-size values were $\mu_w = 2 \times 10^{-6}$, $\mu_b = 10^{-4}$ and $\mu_a = 10^{-5}$.

Fig. 5 shows the power spectra of the three STFS inputs $t_i(n)$ in steady state. The self-interference shows as a ripple effect in the input power spectrum, roughly given by the inverse of the loop delay, i.e. $1/1.6 = 0.625$ MHz. This effect, if not mitigated (and assuming that relay oscillation and/or instability can be avoided in the first place by means of adaptive gain control), may hamper link performance at the final destination, since it can be seen as a multipath channel with very long time spread. In single-carrier systems, this effect will heavily strain the equalizer/decoder module, whereas in multicarrier-based networks it may well result in an effective channel duration exceeding the cyclic prefix, thus resulting in inter-block interference. Clearly, it is preferrable to deal with relay self-interference at the relay station itself by means of feedback cancellation schemes as the one presented here.

Fig. 6 shows the power spectrum of the output signal $y(n)$ in steady state, overlaid on the reference spectrum of the desired signal. It is clear that the adaptive algorithm has effectively suppressed self-interference and even compensated for multipath distortion, while approximately maintaining the same value of SNR encountered at the STFS input.

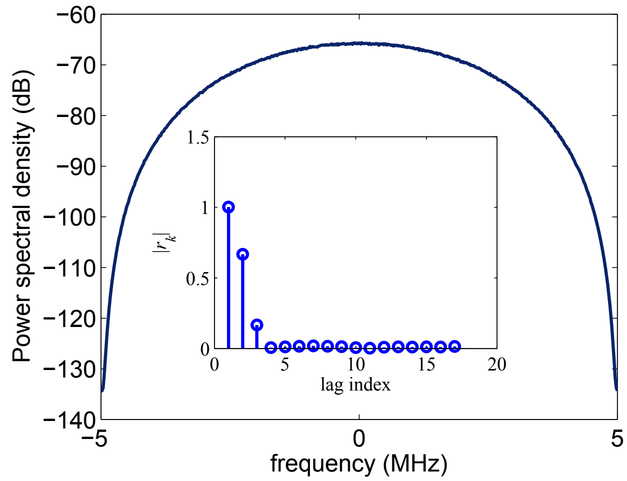

Fig. 3. Power spectrum of $s(n)$ and autocorrelation constants $\{r_k\}$.

6. CONCLUSIONS

We have presented an adaptive algorithm for self-interference suppression in full-duplex relays combining spatial and temporal processing. The spatial processing block is an adaptive MVDR beamformer, whereas the update of the temporal processing block is based on a recently proposed spectrum shaping adaptive scheme for single-input single-output relays. Simulation results attest to the good behavior of the proposed method, which is computationally simple and has the capability to partially mitigate multipath effects in the source-to-relay channel. The a priori knowledge required by the adaptive scheme is the power spectral density and the direction of arrival of the desired signal. Whereas the former can be safely assumed known, it is of interest to derive processing algorithms jointly performing blind angle of arrival estimation and simultaneous self-interference suppression. Future research will be devoted to this goal, together with a deeper analysis of stationary points and their convergence properties.

7. REFERENCES

[1] R. Pabst et al., "Relay-based deployment concepts for wireless and mobile broadband radio," *IEEE Commun. Mag.*, vol. 42, no. 9, pp. 80–89, 2004.

[2] F. Fitzek and M. Katz, Eds., *Cooperation in wireless networks: principles and applications*, Springer, 2006.

[3] A. Sendonaris, E. Erkip, and B. Aazhang, "User cooperation diversity – parts I & II," *IEEE Trans. Commun.*, vol. 51, no. 11, pp. 1927–1948, 2003.

[4] J. N. Laneman, D. N. C. Tse, and G. W. Wornell, "Cooperative diversity in wireless networks: Efficient pro-

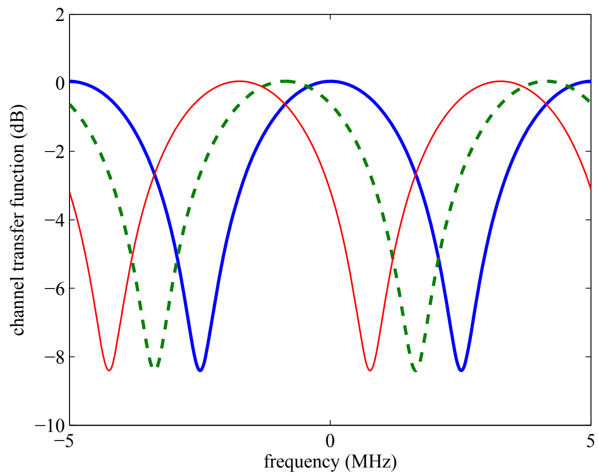

Fig. 4. Transfer function of the propagation channel $\boldsymbol{d}(\omega)$.

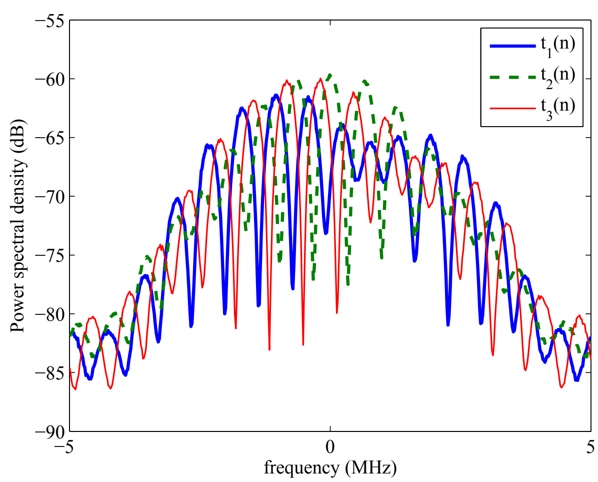

Fig. 5. Power spectra of the signals at the input of the STFS.

tocols and outage behavior," *IEEE Trans. Inf. Theory*, vol. 50, no. 12, pp. 3062–3080, 2004.

[5] P. Larsson and M. Prytz, "MIMO on-frequency repeaterwith self-interference cancellation and mitigation," in *Proc. IEEE 69th Veh. Technol. Conf.*, Apr. 2009.

[6] P. Lioliou, M. Viberg, M. Coldrey, and F. Athley, "Self-interference suppression in full-duplex MIMO relays," in *Proc. Asilomar Conf. Signals, Syst., Comput.*, 2010, pp. 658–662.

[7] T. Riihonen, S. Werner, and R. Wichman, "Mitigation of loopback self-interference in full-duplex MIMO relays," *IEEE Trans. Signal Process.*, vol. 59, no. 12, pp. 5983 –5993, dec. 2011.

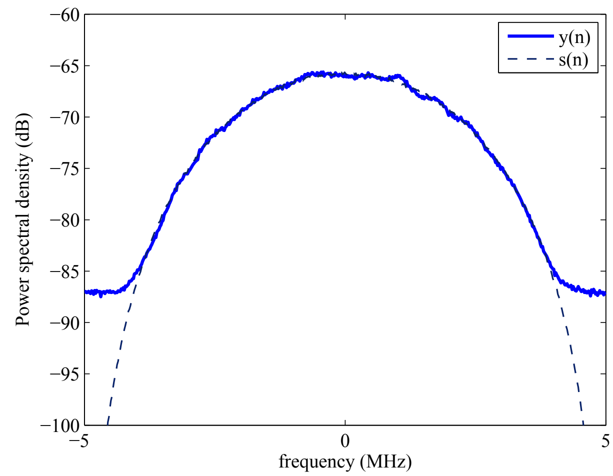

Fig. 6. Power spectrum of the STFS output signal $y(n)$ and reference power spectrum.

[8] R. López-Valcarce, E. Antonio-Rodríguez, C. Mosquera, and F. Pérez-González, "An adaptive feedback canceller for Full-Duplex relays based on spectrum shaping," *IEEE J. Sel. Areas Commun.*, in second round of review.

[9] A. Wiewiorka and P. N. Moss, "Digital on-channel repeater for DAB," *BBC R&D white paper*, , no. WHP120, 2005.

[10] B. Chun et al., "Pre-nulling for self-interference suppression in full-duplex relays," in *Proc. APSIPA Ann. Summit and Conf.*, Oct. 2009.

[11] S. Berger et al., "Recent advances in amplify-and-forward two-hop relaying," *IEEE Commun. Mag.*, vol. 47, no. 7, pp. 50–56, 2009.

[12] A. M. Sayeed, "Deconstructing multiantenna fading channels," *IEEE Trans. Signal Process.*, vol. 50, no. 10, pp. 2563–2579, 2002.

[13] D. G. Manolakis, V. K. Ingle, and S. M. Kogon, *Statistical and adaptive signal processing*, McGraw-Hill, 2000.

[14] T. Engin Uncer and B. Friendlander, Eds., *Classical and Modern Direction-of-Arrival Estimation*, Academic Press, 2009.

[15] O.L. Frost III, "An algorithm for linearly constrained adaptive array processing," *Proc. IEEE*, vol. 60, no. 8, pp. 926 – 935, Aug. 1972.